

# Cellular Uptake Mechanisms and Endosomal Trafficking of Supercharged Proteins

David B. Thompson,<sup>1</sup> Roberto Villaseñor,<sup>2</sup> Brent M. Dorr,<sup>1</sup> Marino Zerial,<sup>2</sup> and David R. Liu<sup>1,\*</sup><sup>1</sup>Howard Hughes Medical Institute, Department of Chemistry and Chemical Biology, Harvard University, 12 Oxford Street, Cambridge, MA 02138, USA<sup>2</sup>Max Planck Institute of Molecular Cell Biology and Genetics, Pfotenhauerstrasse 108, 01307 Dresden, Germany

\*Correspondence: drliu@fas.harvard.edu

<http://dx.doi.org/10.1016/j.chembiol.2012.06.014>

## SUMMARY

Supercharged proteins (SCPs) can deliver functional macromolecules into the cytoplasm of mammalian cells more potently than unstructured cationic peptides. Thus far, neither the structural features of SCPs that determine their delivery effectiveness nor their intracellular fate postendocytosis, has been studied. Using a large set of supercharged GFP (scGFP) variants, we found that the level of cellular uptake is sigmoidally related to net charge and that scGFPs enter cells through multiple pathways, including clathrin-dependent endocytosis and macropinocytosis. SCPs activate Rho and ERK1/2 and also alter the endocytosis of transferrin and EGF. Finally, we discovered that the intracellular trafficking of endosomes containing scGFPs is altered in a manner that correlates with protein delivery potency. Collectively, our findings establish basic structure-activity relationships of SCPs and implicate the modulation of endosomal trafficking as a determinant of macromolecule delivery efficiency.

## INTRODUCTION

The vast majority of nucleic acids and proteins encoded by the human genome are intracellular. Molecular strategies to perturb the function of most biological targets for research or therapeutic purposes, therefore, require agents that can enter cells. Although membrane-permeable small molecules have dominated therapeutics over the past several decades, the use of macromolecules to address biomedical targets has more recently become a focus of intense research (Leader et al., 2008), resulting in a number of macromolecular human drugs (Overington et al., 2006). Macromolecules can offer significant advantages over traditional small molecule-based therapeutics. Macromolecules possess sizes and folding energies that are ideal for catalyzing chemical reactions, potently and selectively binding to extended target surface areas, and encoding gene products. These key features, juxtaposed with the inability of virtually all macromolecules to spontaneously enter cells, create an urgent need to develop effective and general methods for the delivery of functional proteins and nucleic acids into mammalian cells (Schaffert and Wagner, 2008; Gu et al., 2011).

Although a host of protein delivery methods has been developed over the past decade—most notably those based on cationic cell-penetrating peptides (CPPs) (Wadia and Dowdy, 2003; Heitz et al., 2009), but also including antibodies (Song et al., 2005), receptor ligands (Rizk et al., 2009), nanoparticles (Hasadsri et al., 2009), and virus-like particles (Voelkel et al., 2010)—these approaches have not achieved widespread use, and modestly successful protein delivery has historically required high doses of purified protein. We recently developed a platform for macromolecule delivery *in vitro* and *in vivo* based on supercharged proteins (SCPs) (Cronican et al., 2010, 2011; McNaughton et al., 2009). SCPs possess extremely high-positive theoretical net charge at their surfaces, and candidate SCPs can be generated computationally from native, non-SCPs (Lawrence et al., 2007). Proteins can be mutated into SCPs without necessarily abolishing the protein's native structural or functional properties (Lawrence et al., 2007). Recently, we identified a class of naturally occurring supercharged human proteins with theoretical net charge:molecular weight ratios similar to those of engineered SCPs (Cronican et al., 2011). These naturally occurring human SCPs exhibit potent cellular uptake and macromolecule delivery properties similar to engineered SCPs. When compared to the most commonly used CPPs and commercial nucleic acid delivery reagents, SCPs can result in more effective protein and nucleic acid delivery across a range of cell and tissue types *in vitro* and *in vivo* (Cronican et al., 2010, 2011; McNaughton et al., 2009).

The molecular mechanisms by which SCPs enter and are trafficked in cells are largely unknown. Previous studies suggest that cell entry of SCPs shares some mechanistic features with that of other cationic delivery reagents (McNaughton et al., 2009), such as binding to sulfated proteoglycans to mediate initial cellular association, followed by endocytosis and some degree of endosomal escape to the cytosol. However, SCPs can be more efficient at achieving both cell entry and functional macromolecule delivery to the cytosol than CPPs (Cronican et al., 2010; McNaughton et al., 2009). To our knowledge, it is not understood whether the high-delivery potency of SCPs compared with CPPs results solely from the higher theoretical net charges attained by SCPs or from the globular, structured nature of SCPs compared with much shorter and less-structured peptide tags. Observations that support the latter hypothesis include (1) increasing the theoretical net charge of CPPs beyond approximately +15 typically does not increase, and eventually decreases, their cell penetration potency (Mitchell et al., 2000); (2) substitution of arginines on the surfaces of small proteins has been shown to

endow these proteins with cell-penetrating abilities (Daniels and Schepartz, 2007) beyond those of similarly charged cationic peptides; (3) the cell penetration capabilities of oligoarginine peptides have been enhanced by the introduction of disulfide bonds that presumably stabilize the three-dimensional structure of the cationic peptide (Lee et al., 2011); (4) introducing spacer sequences between cationic residues throughout an oligoarginine peptide has also been shown to increase the effectiveness of cellular uptake (Rothbard et al., 2002); and (5) the distribution of cationic residues on the surface of proteins, and not merely charge magnitude, has been shown to alter the effectiveness of certain cell-penetrating proteins (Turcotte et al., 2009). Consistent with these findings, we have observed that SCPs exhibit more potent cell penetration and nucleic acid delivery abilities than synthetic peptides of similar or even greater positive theoretical net charge (McNaughton et al., 2009).

In this work we investigate in detail the role of theoretical net charge and charge distribution on the cellular uptake and delivery properties of SCPs using supercharged GFP (scGFP) as a model. We examined the extent to which SCPs and CPPs alter endocytic processes using a wide range of biochemical assays and high-throughput confocal microscopy. We find that cellular uptake and delivery potencies are strongly charge dependent and that SCPs outperform unstructured peptides of similar charge. We further find that delivery potency correlates with the activation of specific cellular signaling markers, altered endocytosis, and subcellular trafficking. These findings provide mechanistic insights into the unusual ability of SCPs to enter cells and deliver macromolecules, and inform the future development and application of these agents.

## RESULTS

### Effect of Charge Magnitude on Cellular Uptake

Previously, we observed that the CPPs Tat, Arg<sub>10</sub>, and penetratin delivered protein into cells with up to 100-fold lower potencies than that of +36 GFP (Cronican et al., 2010) and that protein and nucleic acid delivery efficiencies mediated by three scGFP variants (+15, +25, and +36 GFPs) correlated with their theoretical net charge (McNaughton et al., 2009). These observations prompted us to characterize in detail (1) the relationship between net theoretical charge and cellular uptake potency, and (2) the effect of charge distribution, either across the surface of a protein or within an unstructured peptide tag, on cellular uptake and delivery potency.

To elucidate these relationships, we generated a collection of 28 scGFP variants with a wide range of theoretical net charges as well as different patterns of charge distribution (see Figure S1 available online). Genes encoding the variants were constructed by combining DNA fragments derived from the coding sequences of previously developed GFPs: stGFP (starting GFP, a nonsupercharged variant), +15 GFP, +25 GFP, +36 GFP, and +48 GFP (Lawrence et al., 2007). Each resulting scGFP variant was expressed and purified from *E. coli* cells. The absorbance and fluorescence emission spectra of all 28 scGFPs were very similar (Figure S2), enabling us to use fluorescence to directly compare the cellular uptake of these proteins.

To determine the relationship of charge-to-cell uptake, each scGFP variant was incubated with HeLa cells for 4 hr across

a range of concentrations. Following incubation, cells were washed using conditions previously shown to remove excess noninternalized protein (Cronican et al., 2010, 2011; McNaughton et al., 2009), trypsinized, and assayed for protein uptake by flow cytometry. For comparison, Tat-stGFP and a GFP engineered by Raines and coworkers to contain an arginine patch (Fuchs and Raines, 2007) were also incubated with HeLa cells and processed in an identical manner. The degree of cellular uptake was measured as the median cellular fluorescence of the population of cells. The relationship of theoretical net charge-to-cellular uptake was found to be strongly sigmoidal and consistent across doses ranging from 20 nM to 2  $\mu$ M (Figure S3). Low-potency uptake, comparable to that of Tat peptide, was observed among proteins with a net theoretical charge less than  $\sim$ +20. In contrast a high-potency regime exhibiting 100-fold higher cellular uptake potency was observed for highly charged proteins (Figure 1A). For GFP the inflection point between the low- and high-potency regimes occurs at a theoretical net charge of approximately +22 (Figure 1A, green points), well above the net charge of CPPs. As this net charge versus cellular uptake relationship predicts, Tat-stGFP (+1 theoretical net charge) exhibited potency comparable to that of other modestly charged, low-potency charged GFP variants, including the Arg-grafted GFP (Fuchs and Raines, 2007) (Figure 1A). The striking change in cell penetration effectiveness from low- to high-potency variants suggests that these variants may enter cells through the involvement of different cellular interactions or through distinct uptake pathways.

### Effect of Charge Distribution on Cellular Uptake

To examine the effect of SCP charge distribution on cell penetration, we generated a series of scGFPs that alter charge distribution without varying theoretical net charge, which was maintained at approximately +25 and +36. The variants within this series were constructed from segments of +48 GFP together with segments of +15 GFP and +25 GFP and, therefore, contained a more uneven cationic charge distribution than canonical +25 or +36 GFPs, with basic residues concentrated into more limited regions of the protein surface. We observed significantly different levels of cellular uptake potencies among scGFPs with similar or identical theoretical net charges but different charge distribution patterns (Figure 1B, red points). These results confirm that the distribution of cationic groups on the surface of a SCP, and not simply the theoretical net charge of the protein, contributes to its cellular uptake properties.

To account for the possibility that interaction between densely substituted cationic residues influences their protonation state and the net charge of scGFPs, we performed cation exchange and found that all proteins eluted in a manner consistent with their relative theoretical net charge rather than with their observed level of cellular uptake (Supplemental Experimental Procedures; Figure S4). Additionally, we tested whether the voltage of the scGFPs was affected by the distribution of charged residues and found that some of the uptake deficiencies of weakly performing scGFPs can be accounted for using a model that describes the electric field of a protein in solution (Supplemental Experimental Procedures; Figure S5).

Taken together, these findings are consistent with a model in which at least one cellular uptake potency-determining event,

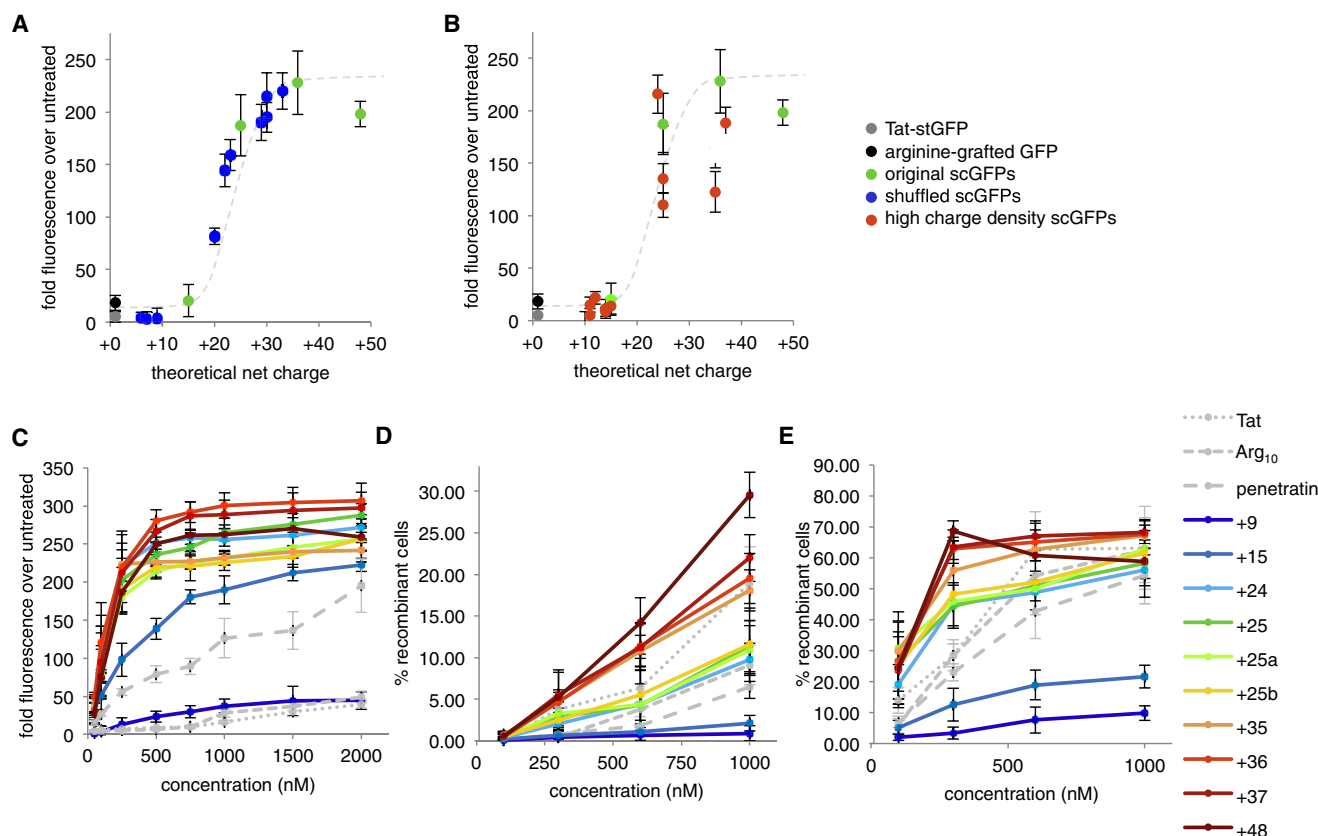


**Figure 1. Charge Dependence of Cellular Uptake and Protein Delivery of scGFPs**

(A) and (B) HeLa cells were treated with 200 nM of each purified scGFP for 4 hr, washed to remove surface-bound protein, and analyzed by flow cytometry. Plots show fold median GFP fluorescence intensity relative to untreated control cells. Blue points represent scGFPs generated by shuffling stGFP, +15 GFP, +25 GFP, and +36 GFP sequences. Red points represent scGFPs generated by shuffling stGFP, +15 GFP, +25 GFP, +36 GFP, and +48 GFP sequences to create proteins with less even charge density. Green points represent starting +15, +25, +36, and +48 GFPs. The gray point is Tat-stGFP (Cronican et al., 2010), and the black point is an arginine-grafted GFP (Fuchs and Raines, 2007).

(C) HeLa cells were treated with the indicated scGFP-mCherry for 4 hr, washed, and analyzed as in part (A). The plot shows median mCherry fluorescence of cells relative to untreated cells.

(D) BSR.LNL.tdTomato Cre reporter cells were treated with scGFP-Cre fusions for 4 hr, washed, incubated an additional 48 hr, and assayed by flow cytometry.

(E) BSR.LNL.tdTomato reporter cells were treated and analyzed exactly as in (D) except that 100  $\mu$ M chloroquine was added during the 4 hr protein incubation and for an additional 12 hr after washing.

Error bars represent the SD of five (A–C) or three (D and E) experiments.

See also Figures S1, S2, S3, S4, S5, S11, and S12.

such as proteoglycan binding or receptor crosslinking (Nakase et al., 2007), is dependent on the arrangement of cationic groups on the surface of a SCP, and not simply on its net charge.

### Charge Dependence of scGFP-Mediated Protein Delivery

The cell penetration properties of macromolecule delivery agents can depend strongly on the associated cargo (Cronican et al., 2010). To determine whether the observed charge-uptake relationship for scGFPs is sustained for scGFP-mediated delivery of fused proteins, a subset of scGFPs was fused to either mCherry or to Cre recombinase (Shaner et al., 2004; Guo et al., 1997). GFPs with theoretical net charges of +9, +15, +24, +25 (three variants designated +25, +25A, and +25B), +35, +36, +37, and +48 were chosen as fusion partners to cover a range of theoretical net charges and to include

some variants with altered charge distributions that performed below the level predicted by their theoretical net charge alone. For comparison the CPPs Tat, Arg<sub>10</sub>, and penetratin were also prepared as fusions with mCherry and Cre recombinase.

HeLa cells were incubated with mCherry fusions for 4 hr at 50 nM to 2  $\mu$ M, washed, and analyzed by flow cytometry using mCherry fluorescence as a measure of protein delivery. The mCherry fusions retained the same general trend of charge-dependent cellular uptake observed for scGFPs alone, with low-potency delivery transitioning to high-potency delivery (up to 50-fold more potent) for variants with >+15 theoretical net charge (Figure 1C). We also observed lower cell penetration potency of the same high-charge variants that underperformed in the cellular uptake study described above (+25A, +25B, +35, +37, and +48 GFPs) (Figure 1C). Fusions with CPPs performed as previously observed, with low overall

mCherry delivery potency comparable to that of the +9 GFP-mCherry fusion, except for penetratin-mCherry, which resulted in moderate levels of delivery at the highest concentrations tested (1–2  $\mu$ M).

Next, we used scGFP-Cre recombinase fusions to assay the functional delivery of protein enzymes to the cytosol. BSR.LNL.tdTomato cells (Cronican et al., 2010) were used to report Cre-dependent recombination. Because scGFP-Cre fusions have little or no recombinase activity until the scGFP moiety is cleaved from the recombinase moiety, we first digested the purified proteins with the endosomal protease cathepsin B to cleave the linker between scGFP and Cre and assayed the resulting proteins in vitro as previously described by Cronican et al. (2010). All cathepsin B-digested scGFP-Cre fusions exhibited recombinase activities comparable to that of wild-type Cre (Figure S6). In addition to being cleaved from scGFP, delivered Cre recombinase must also tetramerize, escape endosomes, translocate to the nucleus, and recombine the reporter gene cassette to trigger tdTomato reporter gene expression. Cells were incubated with each of the scGFP-Cre fusions across a range of concentrations for 4 hr, washed to remove noninternalized proteins as before, then incubated further in protein-free media for 48 hr.

The percentage of recombinant cells resulting from each treatment was revealed by flow cytometry. The Tat, Arg<sub>10</sub>, and penetratin Cre fusions exhibited functional recombinase delivery efficiencies in the low-potency regime, consistent with previously reported results by Cronican et al. (2010, 2011). Functional Cre delivery by scGFPs, in contrast to mCherry delivery, was strictly charge-dependent, with higher-charged scGFPs producing more recombinant cells and like-charged variants clustering together (Figure 1D). Interestingly, variants that were observed to be internalized with significantly lower efficiency than +36 GFP, such as +37 GFP and +48 GFP, when fused to Cre resulted in comparable or even greater recombinant cells than +36 GFP, respectively. The differences between the cellular uptake potencies of these scGFPs (Figure 1C) and their strictly charge-dependent ability to deliver functional Cre (Figure 1D) suggest that protein-intrinsic factors downstream of internalization, such as cleavage of the fusion or endosomal escape efficiency, are potency limiting in the latter case.

To test these possibilities, Cre delivery was repeated in the presence of chloroquine, a small molecule that enhances endosomal escape and increases functional delivery potency of SCPs (Cronican et al., 2010). Importantly, the profile of charge- and dose-dependent Cre recombination (Figure 1D) is significantly shifted toward greater functional delivery in the presence of 100  $\mu$ M chloroquine (Figure 1E) and closely reflects the pattern of total fusion protein uptake (Figure 1C). To probe potential differences in cleavage efficiency of Cre fused to different SCPs, we subjected +15 GFP-Cre and +36 GFP-Cre to in vitro and cell-based cleavage assays. Both proteins were found to be equally cleavable (Figures S7A and 7B), suggesting that proteolytic cleavage efficiency is not a determinant of the differently observed functional delivery abilities. We also assayed the effect of blocking cleavage by coincubation of BSR reporter cells with +36 GFP-Cre and a broad cathepsin inhibitor, Z-Phe-Gly-NHO-Bz (Demuth et al., 1996). At low doses (0.1–0.5  $\mu$ M), there

is a clear depression of delivery (Figure S8), presumably due to a failure to liberate Cre from +36 GFP. At high doses (2–100  $\mu$ M), the efficiency of Cre delivery is dramatically improved (Figure S8), possibly due to continued inhibition of endosomal proteases that would otherwise degrade Cre.

Taken together, these results suggest that functional protein delivery by scGFPs is charge-dependent and protease-dependent and that this dependence is at least partially the result of postinternalization processes. Processes that are likely to influence the intracellular survival and functional delivery of a protein, such as endosomal trafficking, maturation, or escape, may therefore be affected by the presence of highly cationic molecules within endosomes, a hypothesis explored in the experiments below.

### Comparing Delivery Potencies of scGFPs and Similarly Charged Cationic Peptides

The aforementioned studies implicate theoretical net charge as a strong determinant of cell penetration and protein delivery potency. Next, we sought to determine the effect of protein structure on cellular uptake and protein delivery potency by measuring the delivery efficiency of proteins fused to Arg- and Lys-rich peptides with Lys/Arg content comparable to that of scGFPs. Because genes encoding simple fusions of mCherry or Cre to polycationic Arg or Lys peptides longer than ten amino acids did not express efficiently in *E. coli*, we used an enzyme-mediated protein ligation strategy to generate these proteins. The synthetic peptides (KKR)<sub>3</sub>R, (KKR)<sub>6</sub>KR, and (KKR)<sub>9</sub>KRR were efficiently conjugated to mCherry and Cre using a highly active mutant sortase enzyme recently evolved in our laboratory (Supplemental Experimental Procedures) (Chen et al., 2011). The resulting poly-Lys/Arg-fused mCherry and Cre proteins were incubated with reporter cell lines as described above. For comparison, cells were also treated with mCherry and Cre fused to +9, +15, +25, or +36 GFP, which collectively span the range of theoretical net charges covered by the poly-Lys/Arg-fused proteins. Cellular uptake and protein delivery potencies were quantitated by flow cytometry as before.

For mCherry delivery, scGFP fusions consistently outperformed fusions with similarly charged poly-Lys/Arg-conjugated mCherry (Figure 2A). This difference was especially pronounced at lower concentrations. Although at higher concentrations fusions with +20 and +30 peptides approached the performance levels of fusions with +25 GFP, in most cases and at most concentrations, scGFPs resulted in more mCherry delivery than both similarly charged and more highly charged cationic peptides (Figure 2B). These results indicate that scGFPs result in distinctly more potent cellular uptake and mCherry delivery than unstructured cationic peptides, even when the scGFP and the cationic peptides possess a similar theoretical net charge.

The results for Cre recombinase delivery were generally consistent with the mCherry delivery results: scGFP-Cre fusions typically outperformed cationic peptide-Cre fusions, especially at lower doses, with the exception of the lower potency +9 and +15 GFPs (Figure 2C). Interestingly, the +20 and +30 poly-Lys/Arg peptides exhibited decreased Cre delivery potency compared with +10 poly-Lys/Arg, which is approximately as effective as Arg<sub>10</sub>-Cre (Figure 1D), despite the fact that all Cre conjugates and fusions were comparably active in vitro following

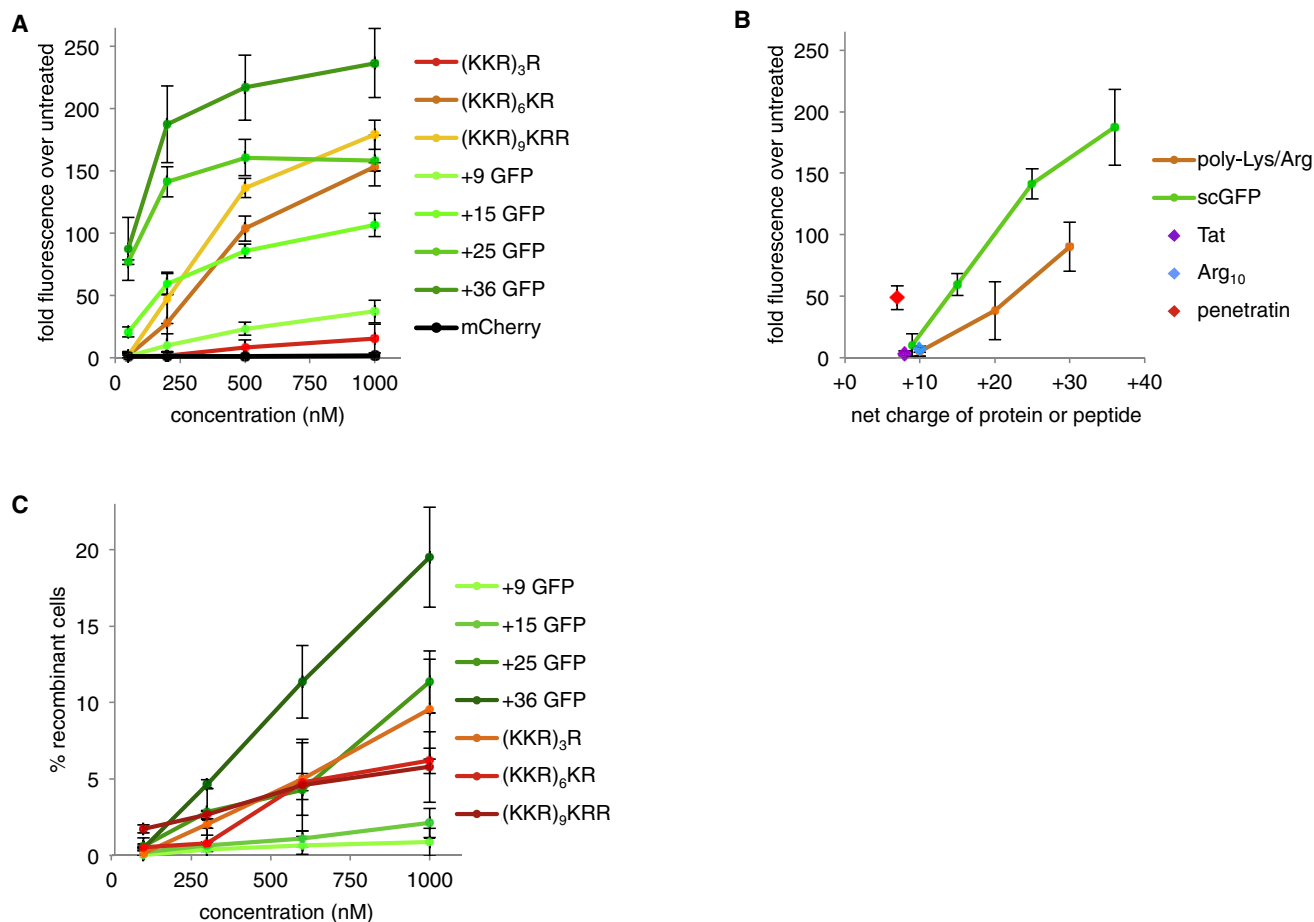


**Figure 2. scGFPs Deliver mCherry and Cre Recombinase More Effectively than Similarly Charged Cationic Peptides**

Cells were treated and analyzed as described in Figure 1C.

(A) Median mCherry fluorescence of cells treated with scGFP-mCherry fusions or cationic peptide-mCherry conjugates at the indicated doses for 4 hr is shown.

(B) mCherry delivery efficiency as a function of protein net charge is presented.

(C) Percent recombinant BSR.LNL.tdTomato reporter cells expressing tdTomato following treatment with scGFP-Cre fusions or cationic peptide-Cre conjugates are shown. Cells were treated and analyzed as described in Figure 1D.

Error bars represent the SD of three experiments.

See also Figures S1, S2, S3, S4, S5, S6, S7, S8, S11, and S12.

cathepsin B treatment (Figure S7) (Cronican et al., 2010). A possible explanation for the lower potency of the +20 and +30 poly-Lys/Arg peptides is their potential cytotoxicity, as has been previously reported for certain cationic peptides and other synthetic cationic polymers (Mitchell et al., 2000; Godbey et al., 1999). This toxicity may not have manifested on the shorter time-scale of the mCherry internalization assays, whereas the Cre assay is necessarily a multiday experiment.

Collectively, these results reveal a cellular uptake and protein delivery-potency advantage from displaying positive charge on a structured protein surface, as is this case with scGFPs, over simply appending the same number of cationic residues in a simple, presumably unstructured peptide tag. This difference may be explained if the higher density of Arg and Lys side chains in a short peptide prevents the complete protonation of every residue by decreasing their pK<sub>a</sub> values to reduce unfavorable charge-charge repulsion, decreasing the actual cationic net charges attainable by synthetic peptides compared with SCPs.

Alternatively, spreading cationic residues over a much larger surface area may engage cell surface receptors or other proteins involved in endocytosis and/or escape from endosomes more effectively than concentrating cationic charge in a small peptide tail. We tested the former possibility using the same cation exchange-based approach that we used to assess the actual charge magnitudes of scGFPs. Poly-Lys/Arg peptides eluted from the cation exchange resin in a manner consistent with their theoretical net charge (Figure S4). These results support a model in which the potency differences between cationic peptides and SCPs arise from differences in their ability to interact with cellular components rather than from differences in their actual versus theoretical net charge.

#### Mechanisms of scGFP Internalization

We previously reported that scGFP uptake is an energy-dependent process that requires actin polymerization and the presence of cell surface-sulfated proteoglycans (McNaughton

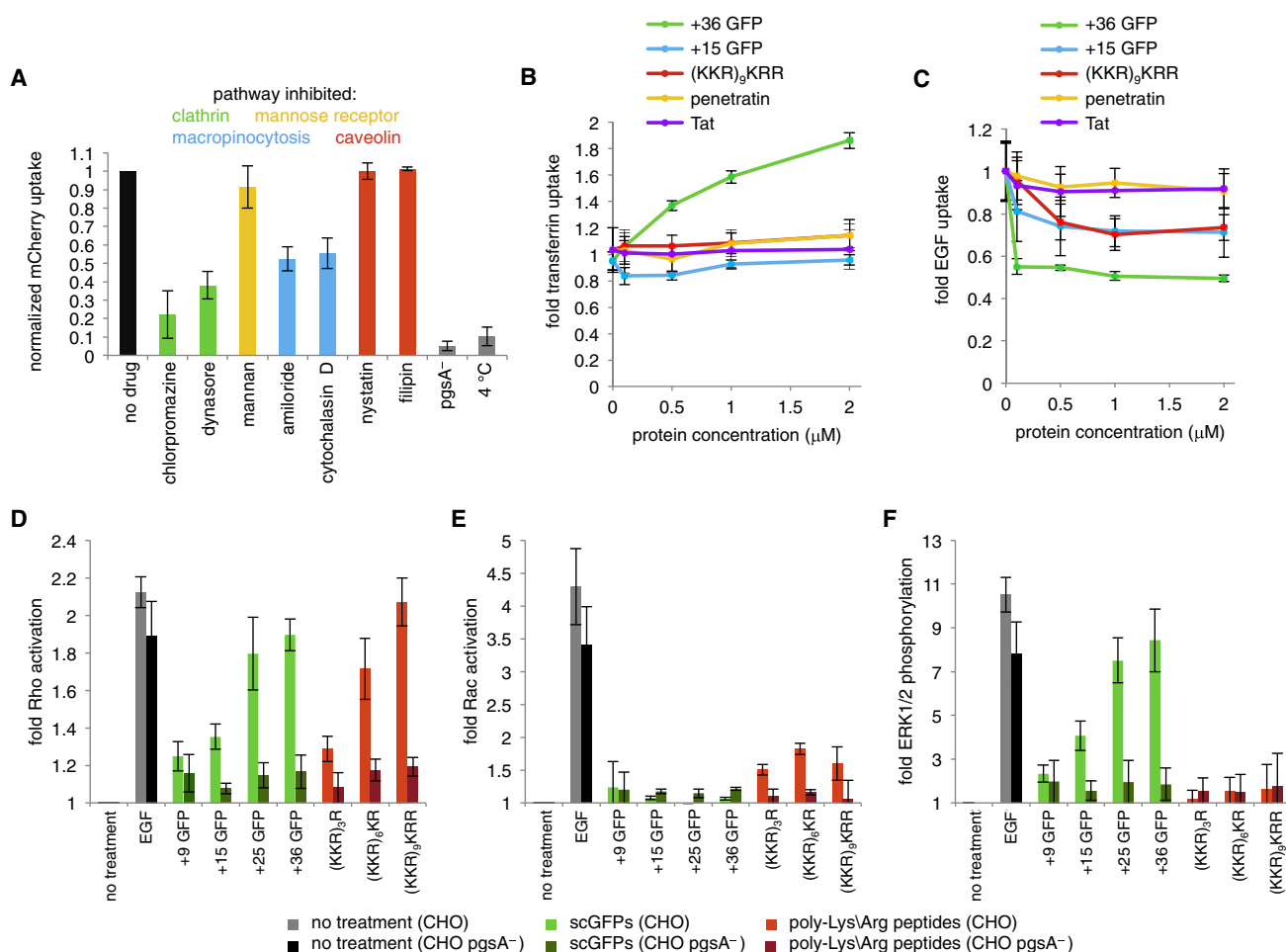


**Figure 3. Endocytic Pathway Probes, Alteration of Transferrin and EGF Uptake, and the Activation of Rho-GTP and ERK1/2 Phosphorylation**

(A) Cells were pretreated for 1 hr with the indicated inhibitor prior to 1 hr treatment with 500 nM +36 GFP in the continued presence of inhibitor, washed, and analyzed by flow cytometry. A mutant cell line, CHO pgsA<sup>-</sup>, which lacks heparin sulfate proteoglycans, and treatment at 4°C instead of 37°C, were included as a control (gray bars).

(B) and (C) HeLa cells cotreated with the indicated cationic protein or peptide for 4 hr and Texas red-labeled transferrin (B), or Alexa 594-labeled EGF (C), were washed and analyzed by flow cytometry. Transferrin and EGF uptake were normalized to cells treated with (B) Texas red-labeled transferrin or (C) Alexa 594-labeled EGF alone.

(D–F) CHO cells (light bars) or CHO pgsA<sup>-</sup> cells (dark bars) were treated with 1 μM of the indicated scGFP or cationic peptide for 5 min prior to washing and harvesting of cell lysate. EGF treatment at 50 ng/ml was included as a control for signaling activation (“EGF”). (D) Rho-GTP quantitation by GLISA is illustrated. (E) Rac-GTP quantitation by GLISA is shown. (F) The extent of ERK1/2 phosphorylation determined by immunoblot with anti-phospho ERK1/2 antibody and quantitated by densitometry is presented.

Error bars represent the SD of three (A and C) or five (D–F) experiments.

See also Figures S1, S2, S9, S10, S11, and S12.

et al., 2009). Given these findings, one possibility is that scGFP may be taken up via macropinocytosis, similar to some CPPs (Wadia et al., 2004; Nakase et al., 2007). In light of the observed cellular uptake and macromolecule delivery differences between scGFPs and cationic CPPs, however, we hypothesized that significant mechanistic differences in their cellular internalization may also exist. We therefore probed the uptake of scGFP in greater detail.

We used a collection of known endocytic inhibitors to probe the role of different endocytic pathways in the uptake of scGFP. HeLa cells were pretreated with each inhibitor for 1 hr prior to incubation with 500 nM +36 GFP and inhibitor for an additional

hour (Figures 3A and S9). Cells were washed as described above, and scGFP uptake was measured by flow cytometry. Amiloride prevents the activation of macropinocytosis (Dangoria et al., 1996), which is implicated in the uptake of cationic CPPs, and inhibits Tat peptide delivery nearly completely at 5 mM (Wadia et al., 2004). In contrast, 5 mM amiloride reduced uptake of scGFP by only 48%. Likewise, cytochalasin D, an inhibitor of actin polymerization, blocked uptake of scGFP by 45% at 10 μM but has been reported to block Tat peptide uptake by >90% (Wadia et al., 2004). These findings suggest that, in contrast to most cationic CPPs, scGFP uptake is not entirely dependent on macropinocytosis and actin-dependent

processes. Interestingly, 5  $\mu\text{g/ml}$  chlorpromazine, which prevents the formation of clathrin-coated pits, and 50  $\mu\text{M}$  dynasore, which prevents the scission of clathrin-coated vesicles (Wang et al., 1993; Macia et al., 2006), inhibited uptake of +36 GFP by 78% and 62%, respectively. Finally, nystatin and filipin, two inhibitors of caveolin-dependent uptake that is involved in the internalization of some viral delivery agents and nonviral protein-based agents (Rothberg et al., 1990, 1992), resulted in no observable impact on scGFP uptake at 50 nM of either inhibitor. These inhibitor studies collectively implicate a clathrin-dependent endocytosis as a major mechanism for the uptake of scGFP and suggest that macropinocytosis plays a lesser role.

To test whether scGFPs modulate clathrin-dependent uptake, we incubated HeLa cells with fluorophore-labeled transferrin, a known clathrin-dependent cargo, and Tat-mCherry, penetratin-mCherry, (KKR)<sub>9</sub>KRR-mCherry, +15 GFP, or +36 GFP at concentrations from 0.1 to 2  $\mu\text{M}$  (Figure 3B). Coincubation with +36 GFP resulted in a marked dose-dependent increase in intracellular transferrin. None of the other proteins tested had an appreciable effect on transferrin uptake. Titration of transferrin (20–200  $\mu\text{g/ml}$ ) in the presence of 200 nM +36 GFP had little effect on +36 GFP uptake, indicating that +36 GFP does not use the same receptor as transferrin but instead stimulates transferrin accumulation independently. We also tested the +35 and +37 GFPs, two proteins that are taken up by cells less efficiently than +36 GFP (Figures 1B and 1C), to see if their lower potency could be explained by a differential effect on the endocytic system but found no appreciable difference in intracellular transferrin levels compared with +36 GFP (Figure S10A). The stimulation of transferrin accumulation by +36 GFP may implicate clathrin in the uptake of scGFP and suggests that high-potency scGFPs potentially alter endocytic processes that rely on this pathway. These results also represent a distinction between high-potency scGFPs and other proteins and peptides tested.

Given the partial inhibition of +36 GFP uptake by the macropinocytosis inhibitor amiloride, we tested the effect of epidermal growth factor (EGF), a known inducer of macropinocytosis, on +36 GFP uptake. Across a range of concentrations (0.1–1  $\mu\text{g/ml}$ ), EGF had no significant impact on +36 GFP uptake (Figure S10B). However, when the internalization of labeled EGF was studied as function of the concentration of +36 GFP, +15 GFP, Tat-mCherry, penetratin-mCherry, and (KKR)<sub>9</sub>KRR-mCherry (0.1–2  $\mu\text{M}$  each), EGF uptake was inhibited by +15 GFP, +36 GFP, and (KKR)<sub>9</sub>KRR-mCherry by up to 40% (Figure 3C). This observation indicates that high-potency cell-penetrant proteins such as +36 GFP may compete with EGF for receptors, strongly induce ligand-independent internalization of EGF receptors (EGFRs) (a known mechanism of EGFR regulation) (West et al., 1989; Goh et al., 2010), or alter EGFR activation, internalization, or degradation through another mechanism. Finally, we examined whether scGFPs damage the cellular membrane, thereby inducing endocytosis via membrane repair pathways (Duchardt et al., 2007). Even at a high dose (10  $\mu\text{M}$ ), +36 GFP does not induce appreciable membrane permeabilization (Figure S11).

Collectively, these mechanistic studies indicate that high-potency scGFPs enter cells through uptake pathways that include clathrin-dependent endocytosis, which may be altered

by scGFPs, and macropinocytosis. Furthermore, scGFPs cause significant changes to the transport of both recycling and degradative endocytic cargoes. Such changes correlate with the potency of protein delivery.

### Rho Activation by scGFPs and Poly-Lys/Arg Peptides

The aforementioned observations suggest that scGFPs enter cells through specific endocytic routes. Next, we characterized the effects of scGFPs on key protein components in endocytosis pathways. Charged peptides including Tat and Arg<sub>10</sub> have been shown to induce the activation of Rac GTPase (Nakase et al., 2007), an early step required for the induction of macropinocytosis. Rho and Rac are GTPases involved in cytoskeletal reorganization and endosomal trafficking (Lua and Low, 2005; Qualmann and Mellor, 2003). Rac is located near the plasma membrane and initiates actin polymerization at the start of macropinosome formation (West et al., 2000). Rho is downstream of multiple endocytic pathways, including caveolin-dependent uptake, and clathrin-independent phagocytosis of particulate matter (Ellis and Mellor, 2000). Rac, on the other hand, is associated with fluid-phase endocytosis (West et al., 2000).

We assayed the activation of the GTP-bound form of Rho and Rac GTPases by scGFPs and poly-Lys/Arg peptides using a colorimetric plate-based “GLISA” (Cytoskeleton). The initial binding events of scGFP and cationic peptides depend on association with sulfated proteoglycans (McNaughton et al., 2009), and the binding and crosslinking of proteoglycans are known to activate endocytosis (Wittrup et al., 2009; Dehio et al., 1998). We therefore used CHO cells as well as mutant CHO pgsA<sup>-</sup> cells defective for xylosyltransferase (Esko et al., 1985), which is responsible for sulfation of proteoglycans, as a control. Cells were incubated for 5 min with proteins, harvested, and lysed. The resulting cell lysates were applied to GLISA plates. Upon treatment with high-potency scGFPs and poly-Lys/Arg peptides, Rho was activated roughly 2-fold compared with untreated controls (Figure 3D). Low-charge variants resulted in significantly lower activation levels, consistent with the observed sigmoidal charge-uptake relationship for scGFP and scGFP-mCherry fusions (Figures 1A and 1C). Treatment of the CHO pgsA<sup>-</sup> cells resulted in low Rho activation across all treatments, indicating that Rho activation is dependent on sulfated proteoglycans (Figure 3D, dark bars). Importantly, the activation of Rho by scGFPs is consistent with our observation of a +36 GFP-dependent intracellular transferrin accumulation (Figure 3B) because Rho plays an important role in clathrin organization, cargo sorting, and endosome motility (Ellis and Mellor, 2000).

We also assayed the activation of GTP-bound Rac by GLISA following treatment with scGFPs or poly-Lys/Arg peptides and observed no activation by scGFPs and weak activation by poly-Lys/Arg peptides (Figure 3E), consistent with observations by others that Rac activation increases following treatment with either Arg<sub>8</sub> or Tat peptides (Nakase et al., 2007). Rho and Rac are known to negatively regulate one another (Sander et al., 1999), and significant Rho activation may depress Rac levels. Given the role of Rho in the activation and maturation of different endocytic pathways (Ellis and Mellor, 2000; West et al., 2000), the aforementioned results could provide a molecular explanation for the scGFP-mediated alteration of transferrin and EGF endocytosis (Figures 3B and 3C).

### ERK1 Activation by scGFPs and Poly-Lys/Arg Peptides

In many cell lines, endocytosis is required for full activation of ERK1/2 following receptor ligation (Pierce et al., 2000; Robertson et al., 2006; Ung et al., 2008). Therefore, changes in ERK1/2 phosphorylation can reflect activation of plasma membrane signaling receptors by scGFPs or changes in the endocytic transport of these receptors (Sorkin and von Zastrow, 2009).

We measured ERK1/2 phosphorylation by immunoblot analysis of cell lysates treated for 5 min with scGFP or poly-Lys/Arg variants to quantitate phospho-ERK1/2 levels. Upon treatment with highly charged scGFPs, but not similarly charged poly-Lys/Arg peptides, cellular ERK1/2 was phosphorylated by up to 8.4-fold over controls lacking treatment (Figure 3F). More modestly charged (+9 or +15) scGFPs also induced ERK1/2 phosphorylation, although to a lower extent (Figure 3F). In all cases tested, ERK1/2 phosphorylation was also dependent on the presence of sulfated proteoglycans, as evidenced by the lack of ERK1/2 phosphorylation in the CHO pgsA<sup>-</sup> cells (Figure 3F, dark bars). This finding suggests that the activation of receptor signaling, and possibly receptor internalization, is an important factor in scGFP uptake. These results also provide additional mechanistic distinctions of scGFP uptake compared with the uptake of unstructured cationic peptides, which have no significant effect on ERK1/2 phosphorylation (Figure 3F).

### Disruption of Endosomal Transport and Maturation by scGFPs and Poly-Lys/Arg Peptides

The amount of material per endosome, the rate of intracellular transport and maturation, and the ultimate destination of endocytosed material are all parameters known to vary among endocytic routes (Collinet et al., 2010). These distinctions can impact the characteristics and effectiveness of protein delivery. A comparison of scGFP uptake, scGFP-mCherry uptake, and functional Cre delivery (Figures 1B–1D) suggests that charge-dependent differences following internalization contribute to the effectiveness of extraendosomal functional delivery of protein cargoes. The high charge of cationic delivery reagents could alter the ionic composition of the endosomal lumen. Because the trafficking of endosomes is closely tied to the function of endosomal membrane ion channels and pumps (Huotari and Helenius, 2011), significant alteration through such a mechanism could disrupt endosome transport and maturation. Endocytosed cargoes targeted for degradation are transported to perinuclear lysosomal compartments within approximately 2 hr (Blanchette et al., 2009). The effective cytosolic delivery of endocytosed material requires that it avoids degradation in the endocytic pathway. A difference in the transport to lysosomes between scGFPs and cationic peptides may explain the observed variations in protein delivery data described above.

We monitored the transport of proteins to lysosomes following internalization by incubation of HeLa cells with 500 nM of a protein of interest for 1 hr. Following this incubation, cells were washed extensively with PBS containing heparin, and incubated a further 4 hr in protein-free media containing heparin to prevent the uptake of any remaining extracellular protein and inhibit the reinternalization of material from recycling endosomes. Dextran, a marker of fluid-phase endocytosis (Oliver et al., 1984), was included as a control. Lysosomes were labeled

with the LysoTracker reagent (Life Technologies), which effectively labels acidified lysosomes.

We performed colocalization analysis of LysoTracker dye with the scGFPs and cationic peptide-tagged mCherry proteins to determine the extent of endosomal trafficking or maturation disruption (Figure 4A). Dextran efficiently colocalized with lysosomes, resulting in a Pearson's correlation coefficient ( $\rho$ ) of 0.8. In contrast all delivered proteins displayed some level of significantly slower transport, with none exhibiting  $\rho > 0.6$ . In all cases, large numbers of protein-containing peripheral endosomes were observed, even 4 hr after removal of the protein reagent from the media. Such a failure to localize to perinuclear acidic vesicles suggests either a slowing of the maturation of protein-containing endosomes or the sorting of scGFPs away from the degradative pathway. The observation of peripheral vesicles was not due to continued or recent internalization of proteins because the cells were incubated in protein-free media following washing and prior to imaging. Likewise, the apparent peripheral distribution was not due to the degradation and disappearance of otherwise perinuclear lysosomal material over time because the total cellular fluorescence did not significantly decrease over the course of the 4 hr incubation following treatment (Figure S6).

The extent of lysosomal colocalization was significantly lower for all scGFPs compared with any cationic peptide tested (Figure 4A). The scGFPs exhibited the least lysosomal colocalization with a trend of decreased lysosomal localization with increased charge (Figure 4A). Within the CPP set of Tat, Arg<sub>10</sub>, and penetratin, the trend of colocalization strongly reflected functional delivery properties, with Tat (the most potent delivery agent of the cationic peptides in this study) exhibiting the lowest lysosomal colocalization. The colocalization data for the poly-Lys/Arg peptides, in contrast, did not follow this trend. Although all poly-Lys/Arg peptides showed significantly reduced lysosomal colocalization compared to dextran, they were among the poorest performing domains in the Cre recombinase delivery assays (Figure 2C). Importantly, the localization of scGFP signal strongly correlates with that of fused proteins of interest, such as Cre, even when the proteins are cleaved (Figure S13).

Collectively, these lysosomal localization results reveal that the relative delivery abilities of scGFPs and CPPs correlate with the extent of slowed endosomal maturation and that scGFP exhibits a stronger effect on these processes than CPPs. That such an effect correlates with the potency of functional delivery suggests that the ultimate nonendosomal fate of delivered proteins relies at least in part on how they are trafficked after internalization.

### Kinetics of scGFP and Cationic Peptide Uptake and Trafficking

After observing the strong effect on endosome transport to lysosomes among the cationic delivery reagents tested, we characterized the events of early endocytosis and tracked differences between scGFPs and CPPs leading up to the observed late-stage endosomal distribution using a recently reported high-throughput confocal microscopy image analysis pipeline (Collinet et al., 2010). This platform enables the measurement of a wide range of endosomal parameters, including trafficking kinetics, endosome number, size distribution, and cargo content.

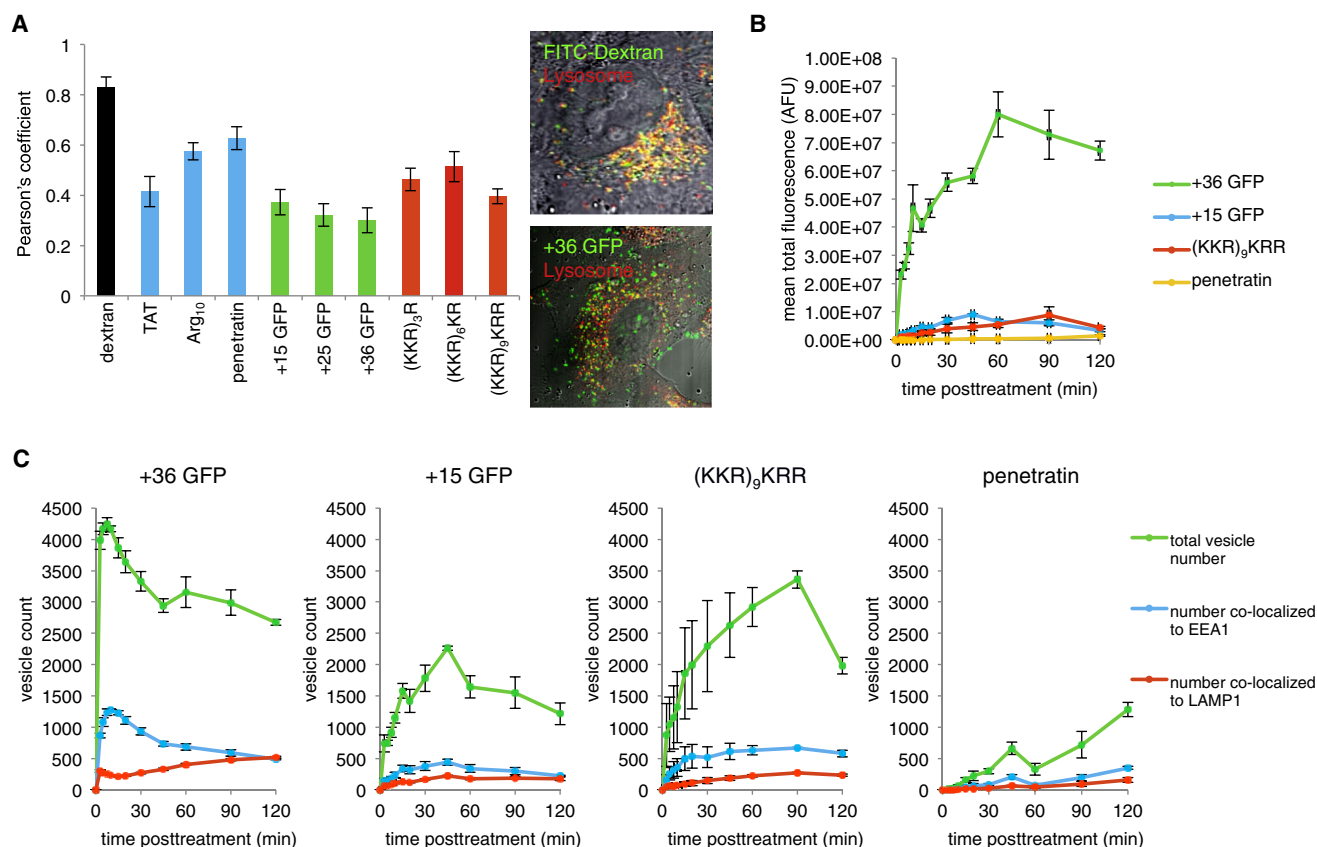


**Figure 4. Uptake and Trafficking Kinetics and Lysosomal Localization of scGFPs and Cationic Peptides**

(A) HeLa cells were treated with 500 nM of scGFPs or peptide-mCherry fusions for 1 hr, washed, incubated an additional 4 hr, and imaged by confocal microscopy. Lysosomes were labeled with LysoTracker Red or Green as appropriate (Life Technologies). The colocalization of proteins with lysosomes was determined by calculation of the Pearson's correlation coefficient of the red and green channels using ImageJ (left). A representative image of cells treated with either FITC-Dextran (top right) or +36 GFP (bottom right) is shown.

(B) and (C) HeLa cells were incubated with the indicated scGFP or peptide-mCherry fusion at 500 nM for up to 2 hr and analyzed by confocal microscopy. (B) The total amount of protein endocytosed over time. (C) Trafficking of protein through early endosomes (labeled with anti-EEA1 antibody; Rink et al., 2005) and lysosomes (labeled with anti-LAMP1 antibody; BD PharMingen) is demonstrated. The number of GFP- or mCherry-containing vesicles showing EEA1 or LAMP1 colocalization was analyzed by high-throughput automated confocal microscopy (Collinet et al., 2010). In all plots, green points represent the total number of vesicles containing scGFP or peptide-mCherry fusions, blue points are vesicles showing EEA1 colocalization, and red points are vesicles showing LAMP1 colocalization.

All error bars represent the SD of 3 experiments, except in (A), which shows the SD from 15 images.

See also Figures S1, S2, S11, S12, S13, S14, S16, and S17.

As representative proteins, we applied this strategy to the study of +36 GFP (a high-potency SCP), +15 GFP (a modestly potent SCP), Tat-mCherry, penetratin-mCherry, and +30 (KKR)<sub>9</sub>KRR-mCherry (three cationic peptides of varying charge and size) (for representative images see Figure S14).

HeLa cells were incubated with 0.1–2 μM of each protein for 30 min, washed, and fixed (Figure S15). Over a range of concentrations, the number of scGFP or CPP-containing vesicles increased steadily (Figure 5A). Among the proteins tested, +36 GFP occupied the highest number of endosomes, even at low concentration (0.1 μM), whereas other proteins did not occupy such a high number of endosomes even at the highest dose (2 μM). The +30 poly-Lys/Arg peptide exhibited a decrease in the number of endosomes formed at high doses. Tat was only detected in a small number of endosomes, consistent with its modest cell uptake potency.

Importantly, over a range of protein concentrations, the amount of protein per endosome did not exhibit a significant dose-dependent increase (Figure 5B). Endosomes with +36 GFP contained roughly 4- to 10-fold more protein per endosome than endosomes with CPPs, whereas +15 GFP-containing endosomes had roughly 2-fold more protein than CPPs. These findings have important implications for interpreting the concentration dependence of functional protein delivery. Although the amount of protein per endosome is likely a factor contributing to the overall effectiveness of protein functional delivery, as evidenced by the relative amounts of protein per endosome for +36 GFP and +15 GFP versus CPPs (Figure 5B), the number of endosomes containing endocytosed protein, rather than the amount of protein per endosome, more closely correlates with dose-dependent changes in functional delivery potency. Increasing the dose of protein during treatments resulted in both more

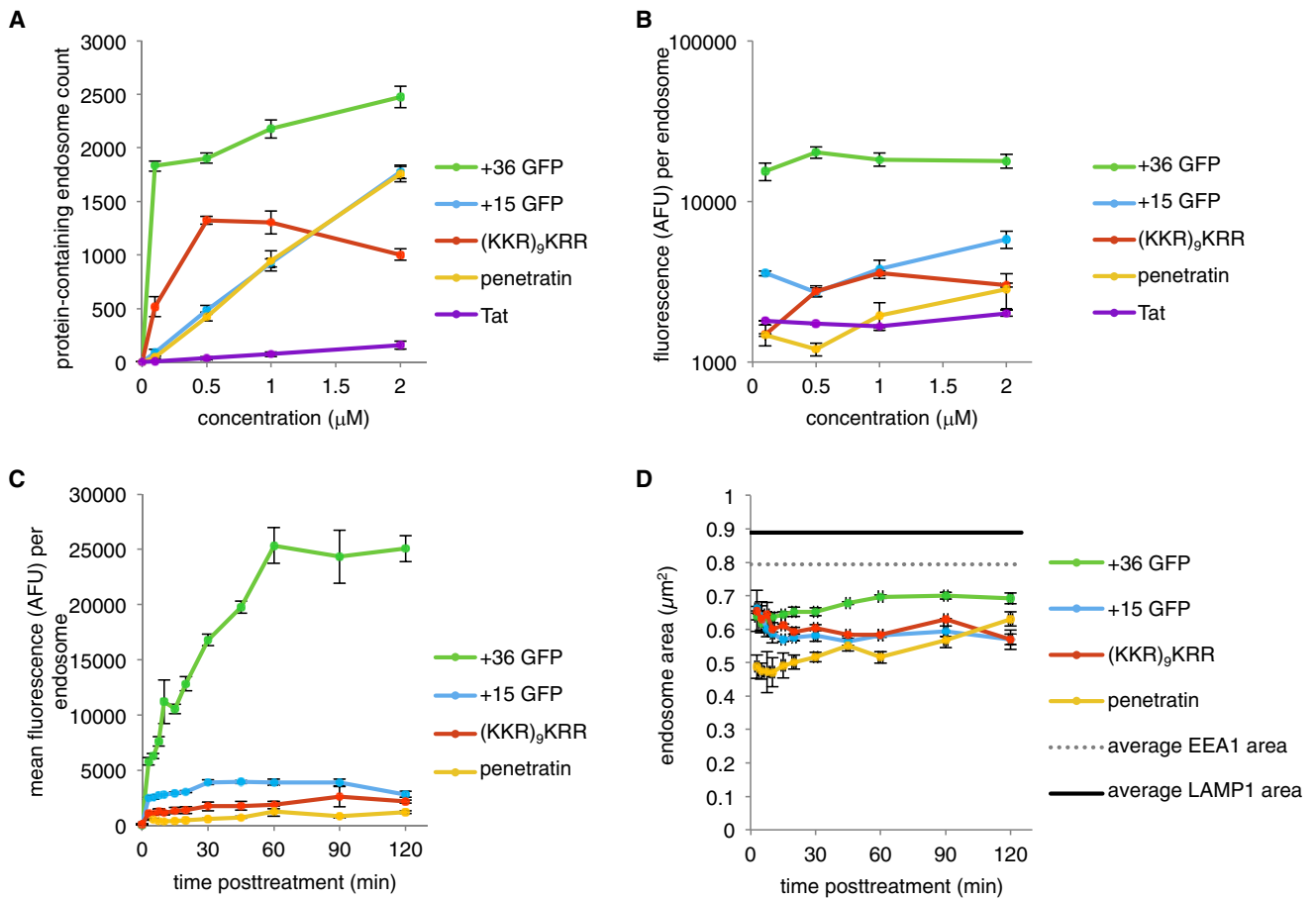


**Figure 5. Effects of scGFPs and Cationic Peptides on Endosome Formation, Endosomal Protein Content, and Endosome Surface Area** (A) and (B) HeLa cells were incubated with the indicated concentrations of scGFP or peptide-mCherry fusion for 1 hr, washed, and the number of GFP or mCherry-containing endosomes was analyzed as in Figures 4B and 4C. (A) SCPs and cationic peptides are endocytosed with greatly different potencies. (B) High-potency scGFPs fill endosomes with more protein than less-potent scGFPs and cationic peptides. (C) and (D) HeLa cells were treated and analyzed exactly as in Figures 4 and 4C. (C) Amount of GFP or mCherry protein per endosome as a function of time is illustrated. (D) Size of endosomes as a function of time, with the average size of early endosomes and lysosomes indicated by the dotted and solid lines, respectively, is shown.

All error bars represent the SD of three experiments. See also Figures S1, S2, S9, S11, S12, S14, S15, S16, and S17.

protein-containing endosomes and more potent functional delivery (Figures 5A and 1D, respectively).

We next measured the uptake and trafficking of proteins over time. Cells were incubated with 500 nM proteins for up to 2 hr. +36 GFP rapidly entered cells, filling a maximal number of early endosomes (identified by the presence of EEA1; Rink et al., 2005) within 10 min of treatment (Figure 4C). The other proteins were much slower in their uptake, requiring as much as 2 hr before reaching maximal early endosome occupancy. Thereafter, +36 GFP quickly exited early endosomal compartments. The rapid uptake and transport to early endosomes of +36 GFP in comparison with the other proteins may reflect the ability of this protein to be mainly internalized by clathrin-mediated endocytosis, as described above (Figure 3A).

Over the course of 2 hr, a small fraction (<20%) of +36 GFP eventually localized to late endosome compartments (identified by the presence of LAMP1) (Figure 4C). Interestingly, the vast majority of +36 GFP is unaccounted for in either of these major

endosomal populations, and the number and size of both populations do not change significantly over time (Figures S16A and S16B). The other proteins tested were slow to enter both early endosomal compartments and late endosomal compartments, whereas a major portion of the protein was retained outside of either of these endosomal populations, as with +36 GFP. The amount of protein degradation postendocytosis, as measured by loss of fluorescence, was not appreciable for any of the proteins within the 2 hr tested. The lack of degradation over this period, and even over a longer 16 hr incubation (Figure S12), suggests a role for dramatically reduced lysosomal degradation in functional protein delivery. Indeed, 80% of the original +36 GFP signal remained within cells after 16 hr, indicating very little proteolysis of the endocytosed cargo. In contrast the intracellular lifetime of other endosomal cargo is comparatively short. For example transferrin can be recycled out of the cell rapidly, with an intracellular half-life of 7 min (Ghosh et al., 1994), EGF is almost completely degraded within

2 hr (Carpenter and Cohen, 1976), and polystyrene beads are transported to lysosomes within 2 hr (Blanchette et al., 2009). The presence of intact protein within an endosomal reservoir for several hours postinternalization may provide a much greater opportunity for these proteins to escape endosomes, even through a low-efficiency mechanism, than endosomal cargoes that are rapidly degraded through canonical pathways.

Finally, we measured the amount of protein per endosome and the size of endosomes over time. These two parameters are indicative of endosomal maturation and fusion and may determine the long-term fate of endocytosed proteins. Over 2 hr the average amount of protein in each cell did not decrease for any protein tested. However, unique among all proteins tested, the number of +36 GFP-containing endosomes decreased sharply (Figure 4C). Consequently, the amount of +36 GFP per endosome increased dramatically over time (Figure 5C). This protein concentration effect was much less pronounced for the other proteins tested, with +36 GFP reaching >5-fold more protein per endosome than any other agent tested, and achieving a 5-fold increase in the amount of protein per endosome over 2 hr. The other agents exhibited a much more modest increase in the amount of protein per endosome during this time (Figure 5C). These measurements suggest that +36 GFP is not significantly inhibiting homotypic fusion and cargo accumulation in endosomes. The size of protein-containing endosomes did not change over time appreciably for any protein tested (Figure 5D), and all endosomes were smaller compared to both early and late endosomes.

These observations suggest a role for the long-term intracellular survival of proteins within a unique peripheral endosomal population during the process of functional protein delivery by SCPs and cationic peptides. The endosomes occupied by +36 GFP are indeed acidified (Figure S17), yet they are not effectively transported to late endosomes (Figure 4C) or lysosomes (Figure 4A). Our observations for +36 GFP may reflect a unique trafficking alteration that is shared at least in part by other polycationic delivery reagents. The specific cause and consequence of these changes are not obvious, but it is possible that a high concentration of cationic moieties within an endosome disrupts luminal ion composition, preventing the maturation of protein-containing endosomes and their subsequent fusion with degradative compartments. If the intraendosomal survival of proteins is extended as a result, then the delivery of functional extraendosomal proteins may strongly depend on such alterations to endosomal trafficking.

## DISCUSSION

In this study we found that the cellular uptake ability of scGFPs exhibits a strong sigmoidal charge dependence. Such a relationship suggests distinct interactions with cellular components or uptake through different endocytic routes by high-charge, high-potency scGFPs compared with CPPs or low-potency scGFPs. Indeed, our subsequent mechanistic studies revealed that high-potency scGFPs alone require clathrin and dynamin for efficient uptake, and modify the transport of clathrin-dependent endocytic cargoes. The potency of scGFPs correlates with the level of activation of Rho and ERK1/2. Such activation may involve the crosslinking of sulfated proteoglycans or other receptors on the cell surface, a process known to induce macro-

pinocytosis by CPPs (Imamura et al., 2011). If receptor crosslinking is indeed the basis of endocytic activation by SCPs, then perhaps the extended surface area provided by highly charged variants explains their greater observed potency compared with more modestly charged scGFPs or unstructured, short cationic CPPs.

The endocytosis inhibitor and transferrin uptake studies described above suggest that scGFP cellular uptake relies significantly on the induction of clathrin-dependent uptake. Although internalization of scGFPs is still dependent on the presence of anionic sulfated proteoglycans, the studies above suggest that the major route of scGFP uptake is not macropinocytosis. These results, combined with the mechanistic studies implicating Rho and ERK1/2 activation, suggest that scGFP uptake likely proceeds through multiple pathways and depends most heavily on a proteoglycan-requiring, clathrin-dependent process.

We observed that both scGFPs and CPPs undergo an altered process of trafficking following endocytosis. The delivery agents tested here are not effectively transported to degradative lysosomal compartments. Moreover, the endocytosed proteins are localized within abnormally small peripheral endosomes that are negative for the early endosome marker EEA1. The magnitude of the changes to endosomal transport correlates with the ability of each reagent to deliver cytosolic proteins. To our knowledge, such changes in transport have not yet been reported for nonviral delivery vehicles and have important implications for the survival of delivered proteins within cells. If protein-containing endosomes fail to mature and efficiently fuse with lysosomal compartments, then delivered proteins may be provided with an extended temporal window during which they can escape into the cytoplasm. Such a phenomenon could contribute to the effectiveness of all cationic delivery vehicles, especially high-potency SCPs, which altered endosome trafficking more than the other proteins and peptides studied here. To our knowledge, the exact mechanism by which scGFPs and CPPs disrupt endosomal transport is not yet understood and represents an attractive subject of future studies. scGFPs also caused significant changes to the transport of the endocytic cargoes transferrin and EGF, raising the possibility that SCPs have multiple effects on specific molecular components of the endocytic system that lead to changes in transferrin receptor and EGFR recycling and degradation.

Together, our findings reveal insights into the mechanism of cellular uptake and trafficking of SCPs and CPPs and more generally highlight the importance of studying at the subcellular level the interaction of delivery agents with their target cells. Such studies improve our understanding of how macromolecule delivery agents work, and identify means by which to optimize their function. These studies also suggest ways in which exposure to such delivery agents can alter cell physiology, an important consideration as macromolecular medicines become increasingly pervasive human therapeutics.

## SIGNIFICANCE

**Supercharged proteins (Cronican et al., 2010, 2011; McNaughton et al., 2009) and other cell-penetrating agents based on folded protein domains (Smith et al., 2008; Daniels and Schepartz, 2007; Fuchs and Raines, 2007) represent an**

**emerging class of macromolecule delivery agents that show improved potency in delivery applications compared to unstructured cationic peptides. In the current study we discovered a highly sigmoidal, ~100-fold charge-dependent increase in cell uptake for highly charged scGFPs above that seen for other cationic delivery agents such as the Tat peptide. This charge-to-cell uptake relationship informs the future identification or engineering of proteins for macromolecule delivery. The differences in endocytic transport by low- and high-charge scGFPs and cationic peptides suggest that intracellular trafficking processes also determine macromolecule delivery potency. Moreover, we have identified an aspect of the interaction between macromolecular delivery agents and their target cells that, to our knowledge, was previously undescribed. Using a detailed analysis of the subcellular endosomal transport of scGFPs and cationic peptides, we found that all of these agents exhibit altered intracellular transport across a number of parameters, and none is as efficiently transported to lysosomes as would be expected for typical endosomal cargo targeted for degradation. Given that lysosomal localization was anti-correlated with functional delivery potency by these proteins, it seems likely that alteration of trafficking is an important postuptake factor in determining delivery potency, perhaps in part by extending their lifetime in cells. In summary this study reveals protein and cellular factors that determine the effectiveness of cationic protein- and peptide-based delivery agents, and implicates specific pathways that may explain their significant potency differences.**

#### EXPERIMENTAL PROCEDURES

Complete experimental procedures are presented in the accompanying Supplemental Experimental Procedures.

#### SUPPLEMENTAL INFORMATION

Supplemental Information includes Supplemental Results, Supplemental Experimental Procedures, and seventeen figures and can be found with this article online at <http://dx.doi.org/10.1016/j.chembiol.2012.06.014>.

#### ACKNOWLEDGMENTS

This work was supported by the National Institutes of Health/NIGMS (R01GM065400 and R01 GM095501), the Howard Hughes Medical Institute, the Virtual Liver initiative (<http://www.virtual-liver.de>) funded by the German Federal Ministry of Research and Education, the Max Planck Society, and the Deutsche Forschungsgemeinschaft. D.B.T. was supported by the Department of Defense through the National Defense Science & Engineering Graduate Fellowship Program. We thank C. Möbius from the High-Throughput Technology Development Studio at the MPI-CBG for assistance with automated image acquisition. D.R.L. is a consultant for Permeon Biologics, a company that has licensed Harvard's intellectual property on macromolecule delivery.

Received: March 9, 2012

Revised: May 17, 2012

Accepted: June 21, 2012

Published: July 26, 2012

#### REFERENCES

Blanchette, C.D., Woo, Y.-H., Thomas, C., Shen, N., Sulchek, T.A., and Hiddessen, A.L. (2009). Decoupling internalization, acidification and

phagosomal-endosomal/lysosomal fusion during phagocytosis of In1A coated beads in epithelial cells. *PLoS One* 4, e6056.

Carpenter, G., and Cohen, S. (1976). 125I-labeled human epidermal growth factor. Binding, internalization, and degradation in human fibroblasts. *J. Cell Biol.* 71, 159–171.

Chen, I., Dorr, B.M., and Liu, D.R. (2011). A general strategy for the evolution of bond-forming enzymes using yeast display. *Proc. Natl. Acad. Sci. USA* 108, 11399–11404.

Collinet, C., Stöter, M., Bradshaw, C.R., Samusik, N., Rink, J.C., Kenski, D., Habermann, B., Buchholz, F., Henschel, R., Mueller, M.S., et al. (2010). Systems survey of endocytosis by multiparametric image analysis. *Nature* 464, 243–249.

Cronican, J.J., Thompson, D.B., Beier, K.T., McNaughton, B.R., Cepko, C.L., and Liu, D.R. (2010). Potent delivery of functional proteins into Mammalian cells in vitro and in vivo using a supercharged protein. *ACS Chem. Biol.* 5, 747–752.

Cronican, J.J., Beier, K.T., Davis, T.N., Tseng, J.-C., Li, W., Thompson, D.B., Shih, A.F., May, E.M., Cepko, C.L., Kung, A.L., et al. (2011). A class of human proteins that deliver functional proteins into mammalian cells in vitro and in vivo. *Chem. Biol.* 18, 833–838.

Dangoria, N.S., Breau, W.C., Anderson, H.A., Cishek, D.M., and Norkin, L.C. (1996). Extracellular simian virus 40 induces an ERK/MAP kinase-independent signalling pathway that activates primary response genes and promotes virus entry. *J. Gen. Virol.* 77, 2173–2182.

Daniels, D.S., and Schepartz, A. (2007). Intrinsically cell-permeable miniature proteins based on a minimal cationic PPII motif. *J. Am. Chem. Soc.* 129, 14578–14579.

Dehio, C., Freissler, E., Lanz, C., Gómez-Duarte, O.G., David, G., and Meyer, T.F. (1998). Ligation of cell surface heparan sulfate proteoglycans by antibody-coated beads stimulates phagocytic uptake into epithelial cells: a model for cellular invasion by *Neisseria gonorrhoeae*. *Exp. Cell Res.* 242, 528–539.

Demuth, H.U., Schierhorn, A., Bryan, P., Höfke, R., Kirschke, H., and Brömme, D. (1996). N-peptidyl, O-acyl hydroxamates: comparison of the selective inhibition of serine and cysteine proteinases. *Biochim. Biophys. Acta* 1295, 179–186.

Duchardt, F., Fotin-Mleczek, M., Schwarz, H., Fischer, R., and Brock, R. (2007). A comprehensive model for the cellular uptake of cationic cell-penetrating peptides. *Traffic* 8, 848–866.

Ellis, S., and Mellor, H. (2000). Regulation of endocytic traffic by rho family GTPases. *Trends Cell Biol.* 10, 85–88.

Esko, J.D., Stewart, T.E., and Taylor, W.H. (1985). Animal cell mutants defective in glycosaminoglycan biosynthesis. *Proc. Natl. Acad. Sci. USA* 82, 3197–3201.

Fuchs, S.M., and Raines, R.T. (2007). Arginine grafting to endow cell permeability. *ACS Chem. Biol.* 2, 167–170.

Ghosh, R.N., Gelman, D.L., and Maxfield, F.R. (1994). Quantification of low density lipoprotein and transferrin endocytic sorting HEP2 cells using confocal microscopy. *J. Cell Sci.* 107, 2177–2189.

Godbey, W.T., Wu, K.K., and Mikos, A.G. (1999). Size matters: molecular weight affects the efficiency of poly(ethyleneimine) as a gene delivery vehicle. *J. Biomed. Mater. Res.* 45, 268–275.

Goh, L.K., Huang, F., Kim, W., Gygi, S., and Sorkin, A. (2010). Multiple mechanisms collectively regulate clathrin-mediated endocytosis of the epidermal growth factor receptor. *J. Cell Biol.* 189, 871–883.

Gu, Z., Biswas, A., Zhao, M., and Tang, Y. (2011). Tailoring nanocarriers for intracellular protein delivery. *Chem. Soc. Rev.* 40, 3638–3655.

Guo, F., Gopaul, D.N., and van Duyn, G.D. (1997). Structure of Cre recombinase complexed with DNA in a site-specific recombination synapse. *Nature* 389, 40–46.

Hasadsri, L., Kreuter, J., Hattori, H., Iwasaki, T., and George, J.M. (2009). Functional protein delivery into neurons using polymeric nanoparticles. *J. Biol. Chem.* 284, 6972–6981.

- Heitz, F., Morris, M.C., and Divita, G. (2009). Twenty years of cell-penetrating peptides: from molecular mechanisms to therapeutics. *Br. J. Pharmacol.* *157*, 195–206.
- Huotari, J., and Helenius, A. (2011). Endosome maturation. *EMBO J.* *30*, 3481–3500.
- Imamura, J., Suzuki, Y., Gonda, K., Roy, C.N., Gatanaga, H., Ohuchi, N., and Higuchi, H. (2011). Single particle tracking confirms that multivalent Tat protein transduction domain-induced heparan sulfate proteoglycan cross-linkage activates Rac1 for internalization. *J. Biol. Chem.* *286*, 10581–10592.
- Lawrence, M.S., Phillips, K.J., and Liu, D.R. (2007). Supercharging proteins can impart unusual resilience. *J. Am. Chem. Soc.* *129*, 10110–10112.
- Leader, B., Baca, Q.J., and Golan, D.E. (2008). Protein therapeutics: a summary and pharmacological classification. *Nat. Rev. Drug Discov.* *7*, 21–39.
- Lee, S.J., Yoon, S.H., and Doh, K.O. (2011). Enhancement of gene delivery using novel homodimeric tat peptide formed by disulfide bond. *J. Microbiol. Biotechnol.* *21*, 802–807.
- Lua, B.L., and Low, B.C. (2005). Activation of EGF receptor endocytosis and ERK1/2 signaling by BPGAP1 requires direct interaction with EEN/endophilin II and a functional RhoGAP domain. *J. Cell Sci.* *118*, 2707–2721.
- Macia, E., Ehrlich, M., Massol, R., Boucrot, E., Brunner, C., and Kirchhausen, T. (2006). Dynasore, a cell-permeable inhibitor of dynamin. *Dev. Cell* *10*, 839–850.
- McNaughton, B.R., Cronican, J.J., Thompson, D.B., and Liu, D.R. (2009). Mammalian cell penetration, siRNA transfection, and DNA transfection by supercharged proteins. *Proc. Natl. Acad. Sci. USA* *106*, 6111–6116.
- Mitchell, D.J., Kim, D.T., Steinman, L., Fathman, C.G., and Rothbard, J.B. (2000). Polyarginine enters cells more efficiently than other polycationic homopolymers. *J. Pept. Res.* *56*, 318–325.
- Nakase, I., Tadokoro, A., Kawabata, N., Takeuchi, T., Katoh, H., Hiramoto, K., Negishi, M., Nomizu, M., Sugiura, Y., and Futaki, S. (2007). Interaction of arginine-rich peptides with membrane-associated proteoglycans is crucial for induction of actin organization and macropinocytosis. *Biochemistry* *46*, 492–501.
- Oliver, J.M., Berlin, R.D., and Davis, B.H. (1984). Use of horseradish peroxidase and fluorescent dextrans to study fluid pinocytosis in leukocytes. *Methods Enzymol.* *108*, 336–347.
- Overington, J.P., Al-Lazikani, B., and Hopkins, A.L. (2006). How many drug targets are there? *Nat. Rev. Drug Discov.* *5*, 993–996.
- Pierce, K.L., Maudsley, S., Daaka, Y., Luttrell, L.M., and Lefkowitz, R.J. (2000). Role of endocytosis in the activation of the extracellular signal-regulated kinase cascade by sequestering and nonsequestering G protein-coupled receptors. *Proc. Natl. Acad. Sci. USA* *97*, 1489–1494.
- Qualmann, B., and Mellor, H. (2003). Regulation of endocytic traffic by Rho GTPases. *Biochem. J.* *371*, 233–241.
- Rink, J., Ghigo, E., Kalaizidis, Y., and Zerial, M. (2005). Rab conversion as a mechanism of progression from early to late endosomes. *Cell* *122*, 735–749.
- Rizk, S.S., Luchniak, A., Uysal, S., Brawley, C.M., Rock, R.S., and Kossiakoff, A.A. (2009). An engineered substance P variant for receptor-mediated delivery of synthetic antibodies into tumor cells. *Proc. Natl. Acad. Sci. USA* *106*, 11011–11015.
- Robertson, S.E., Setty, S.R., Sitaram, A., Marks, M.S., Lewis, R.E., and Chou, M.M. (2006). Extracellular signal-regulated kinase regulates clathrin-independent endosomal trafficking. *Mol. Biol. Cell* *17*, 645–657.
- Rothbard, J.B., Kreider, E., VanDeusen, C.L., Wright, L., Wylie, B.L., and Wender, P.A. (2002). Arginine-rich molecular transporters for drug delivery: role of backbone spacing in cellular uptake. *J. Med. Chem.* *45*, 3612–3618.
- Rothberg, K.G., Ying, Y.S., Kamen, B.A., and Anderson, R.G. (1990). Cholesterol controls the clustering of the glycopospholipid-anchored membrane receptor for 5-methyltetrahydrofolate. *J. Cell Biol.* *111*, 2931–2938.
- Rothberg, K.G., Heuser, J.E., Donzell, W.C., Ying, Y.S., Glenney, J.R., and Anderson, R.G. (1992). Caveolin, a protein component of caveolae membrane coats. *Cell* *68*, 673–682.
- Sander, E.E., ten Klooster, J.P., van Delft, S., van der Kammen, R.A., and Collard, J.G. (1999). Rac downregulates Rho activity: reciprocal balance between both GTPases determines cellular morphology and migratory behavior. *J. Cell Biol.* *147*, 1009–1022.
- Schaffert, D., and Wagner, E. (2008). Gene therapy progress and prospects: synthetic polymer-based systems. *Gene Ther.* *15*, 1131–1138.
- Shaner, N.C., Campbell, R.E., Steinbach, P.A., Giepmans, B.N.G., Palmer, A.E., and Tsien, R.Y. (2004). Improved monomeric red, orange and yellow fluorescent proteins derived from *Discosoma* sp. red fluorescent protein. *Nat. Biotechnol.* *22*, 1567–1572.
- Smith, B.A., Daniels, D.S., Coplin, A.E., Jordan, G.E., McGregor, L.M., and Schepartz, A. (2008). Minimally cationic cell-permeable miniature proteins via  $\alpha$ -helical arginine display. *J. Am. Chem. Soc.* *130*, 2948–2949.
- Song, E., Zhu, P., Lee, S.K., Chowdhury, D., Kussman, S., Dykxhoorn, D.M., Feng, Y., Palliser, D., Weiner, D.B., Shankar, P., et al. (2005). Antibody mediated in vivo delivery of small interfering RNAs via cell-surface receptors. *Nat. Biotechnol.* *23*, 709–717.
- Sorkin, A., and von Zastrow, M. (2009). Endocytosis and signalling: intertwining molecular networks. *Nat. Rev. Mol. Cell Biol.* *10*, 609–622.
- Turcotte, R.F., Lavis, L.D., and Raines, R.T. (2009). Onconase cytotoxicity relies on the distribution of its positive charge. *FEBS J.* *276*, 3846–3857.
- Ung, C.Y., Li, H., Ma, X.H., Jia, J., Li, B.W., Low, B.C., and Chen, Y.Z. (2008). Simulation of the regulation of EGFR endocytosis and EGFR-ERK signaling by endophilin-mediated RhoA-EGFR crosstalk. *FEBS Lett.* *582*, 2283–2290.
- Voelkel, C., Galla, M., Maetzig, T., Warlich, E., Kuehle, J., Zychlinski, D., Bode, J., Cantz, T., Schambach, A., and Baum, C. (2010). Protein transduction from retroviral Gag precursors. *Proc. Natl. Acad. Sci. USA* *107*, 7805–7810.
- Wadia, J.S., and Dowdy, S.F. (2003). Modulation of cellular function by TAT mediated transduction of full length proteins. *Curr. Protein Pept. Sci.* *4*, 97–104.
- Wadia, J.S., Stan, R.V., and Dowdy, S.F. (2004). Transducible TAT-HA fusogenic peptide enhances escape of TAT-fusion proteins after lipid raft macropinocytosis. *Nat. Med.* *10*, 310–315.
- Wang, L.H., Rothberg, K.G., and Anderson, R.G. (1993). Mis-assembly of clathrin lattices on endosomes reveals a regulatory switch for coated pit formation. *J. Cell Biol.* *123*, 1107–1117.
- West, M.A., Bretscher, M.S., and Watts, C. (1989). Distinct endocytotic pathways in epidermal growth factor-stimulated human carcinoma A431 cells. *J. Cell Biol.* *109*, 2731–2739.
- West, M.A., Prescott, A.R., Eskelinen, E.L., Ridley, A.J., and Watts, C. (2000). Rac is required for constitutive macropinocytosis by dendritic cells but does not control its downregulation. *Curr. Biol.* *10*, 839–848.
- Wittrup, A., Zhang, S.H., ten Dam, G.B., van Kuppevelt, T.H., Bengtson, P., Johansson, M., Welch, J., Mörgelein, M., and Belting, M. (2009). ScFv antibody-induced translocation of cell-surface heparan sulfate proteoglycan to endocytic vesicles: evidence for heparan sulfate epitope specificity and role of both syndecan and glypican. *J. Biol. Chem.* *284*, 32959–32967.